50-MeV RUN OF THE IOTA/FAST ELECTRON ACCELERATOR*

D. Edstrom, Jr.#, C. Baffes, C. Briegel, D.R. Broemmelsiek, K. Carlson, B. Chase, D.J. Crawford, E. Cullerton, J. Diamond, N. Eddy, B. Fellenz, E. Harms, M. Kucera, J. Leibfritz, A.H. Lumpkin, D. Nicklaus, E. Prebys, P. Prieto, J. Reid, A. Romanov, J. Ruan, J. Santucci, T. Sen, V. Shiltsev, Y. Shin, G. Stancari, J.C. Thangaraj, R. Thurman-Keup, A. Valishev, A.Warner, S. Wesseln
(FNAL, Batavia, IL), P. Kobak (BYU-I, Rexburg, ID), W. Rush (KU, Lawrence, Kansas),
A. Green, A. Halavanau, D. Mihalcea, P. Piot (NIU, DeKalb, IL, USA)
J. Hyun (Sokendai, Ibaraki, Japan)

Abstract

The low-energy section of the photoinjector-based electron linear accelerator at the Fermilab Accelerator Science & Technology (FAST) facility was recently commissioned to an energy of 50 MeV. This linear accelerator relies primarily upon pulsed SRF acceleration and an optional bunch compressor to produce a stable beam within a large operational regime in terms of bunch charge, total average charge, bunch length, and beam energy. Various instrumentation was used to characterize fundamental properties of the electron beam including the intensity, stability, emittance, and bunch length. While much of this instrumentation was commissioned in a 20 MeV running period prior, some (including a new Martin-Puplett interferometer) was in development or pending installation at that time. All instrumentation has since been recommissioned over the wide operational range of beam energies up to 50 MeV, intensities up to 4 nC/pulse, and bunch structures from ~1 ps to more than 50 ps in length.

INTRODUCTION

The Fermilab Accelerator Science & Technology (FAST) facility team is constructing a 300 MeV electron linac based on superconducting RF (SRF) technology [1]. Once complete, the beamline will be used to inject 150 MeV electrons into the Integral Optics Test Accelerator (IOTA) ring currently being built to test integrable nonlinear inserts [2,3], electron lenses for space-charge compensation [4,5], and other advanced accelerator technologies [6,7]. The low electron injector duty factor required for IOTA (i.e. a single pulse train to be injected on demand every few minutes) allows for a beamline-based test program run in parallel to make use of the large, stable operational parameter space provided by the electron injector as summarized in Table 1. The injector itself comprises a number of components including a photoinjector-based electron gun, a 25-meter-long low-energy (≤50 MeV) beamline shown in Fig. 1, and an 100-meter-long high-energy (≤300 MeV) beamline. The IOTA ring is being built at the end of the high energy section near the high-energy absorber. Here we address commissioning of first beam to the full 50 MeV energy of the low energy beamline to the low energy absorber.

* This work was supported by the DOE contract No.DEAC02-07CH11359 to the Fermi Research Alliance LLC.
# edstrom@fnal.gov

LOW ENERGY BEAMLINE

The electron gun is a normal-conducting, 1.5-cell copper cavity operating at 1.3 GHz. A train of pulsed UV from the drive laser strikes a Cs_2Te-coated Mo cathode in the gun cavity resulting in a train of electron bunches with bunch charge of up to 4 nC/bunch. A 4.5 MeV electron beam from the gun passes through a short (~1 m) low-energy diagnostic section before acceleration in two consecutive superconducting RF structures referred to as capture cavities, CC1 and CC2. Each capture cavity in its own cryostat is a 9-cell, 1.3 GHz (L-Band), Nb accelerating structure cooled nominally to 2 K. Following acceleration, the electron beam passes through the low-energy beam transport section, which includes steering and focusing elements, an optional chicane for bunch compression and beam transforms, as well as a host of instrumentation. It is then directed into the low-energy absorber ahead of the high-energy section still under construction. This begins with a TESLA Type IV ILC-style cryomodule, which has been conditioned previously to 31.25 MeV/cavity to provide ~300 MeV beam to the high-energy absorber, planned for 2017 [1].

Primary instrumentation in the low-energy beamline is named for its position, between 100 and 125, where the gun defines the beginning of the beamline at 100 and the cryomodule defines the end of the low-energy beamline at 126, and it includes beam position monitors (BPMs), two toroids, two wall current monitors, loss monitors, a ceramic gap [8], and transverse profile monitors (TPMs). The last is a modular component that is used to insert a cerium-doped YAG screen or OTR foil into the beam path. The YAG screens and many of the OTR foils are monitored with cameras, allowing for a direct measurement of the transverse electron beam profile, but one of the OTR foils (in the TPM at instrumentation cross X121) provides signal to a Hamamatsu C5680 streak camera and the Martin-Puplett interferometer (MPI).

With the exception of the MPI, the instrumentation noted above had already been used to characterize the electron beam in the 20-MeV low-energy commissioning run in 2015 [9]. In that run, CC1 had not been installed, limiting the energy and presenting a longer drift between the gun and CC2. Measurements made in this commissioning run included beam energy measurements using the path

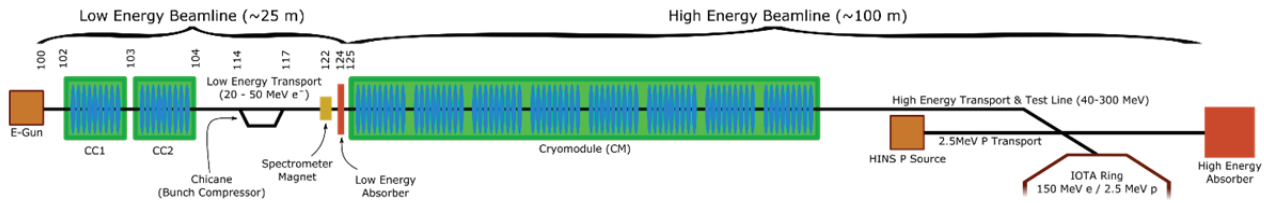

Figure 1: The FAST Accelerator. The FAST low energy beamline was commissioned to 52.5 MeV and the High Energy Transport section is being constructed now.

through an NMR-locked low-energy spectrometer magnet, bunch length measurements made with both the ceramic gap and streak camera, and emittance measurements by means of quadrupole scans. The Z-shaper, a set of three αBBO crystals with independent closed-loop control, was also installed in-line with the UV drive laser [10], allowing for arbitrary pulse shape and length up to 70 ps [11].

Once the 20-MeV run was complete, CC1 was installed allowing for warm coupler conditioning (a sequence in which power is stepped up slowly to process out sources of field emission) to start in mid-February 2016 and concluding on April 15th. Following this CC1 and CC2 were cooled down. A number of issues with the cryogenic system were resolved and the nominal operating point of2 K was reached on May 9th. CC1 and CC2 were then conditioned to an estimated 28 MeV/m and 20 MeV/m respectively. Beam was established to the low-energy absorber with energy of 52.5 MeV through the spectrometer magnet on May 16th, 2016.

50-MEV RUN OVERVIEW

As with the Z-shaper in the 20-MeV run, a test program was implemented for the 50-MeV run, this time primarily dedicated to the crystal channeling radiation experiment [12]. There were difficulties in observing the channeling radiation in the data collected thus far, but a number of issues have been identified should the test be repeated in future running. These issues include alignment considerations and detector constraints, any or all of which may have contributed to lack of detection [9].

Table 1: Summary of primary IOTA/FAST low-energy electron injector beam parameters. Parameters verified previously, but not as part of the 50-MeV run are denoted with an asterisk.

Parameter	FAST Value
Beam Energy	20 MeV – 50 MeV
Bunch Charge	< 10 fC – 3.2 nC per pulse
Bunch Train (Macropulse)	0.5 – 9* MHz for up to 1 ms (3 MHz nominal)
Train Frequency	1 – 5* Hz
Bunch Length	Range: 0.9 – 70* ps (Nom: 5 ps)
Bunch Emittance for 50 pC/pulse	Horz: 1.6 ± 0.2 μm Vert: 3.4 ± 0.1 μm

Intensity

Transmission from the gun to the low energy absorber is nominally monitored as the difference between the intensities recorded at toroids T102 and T124. The toroids were found to be sensitive to 20 pC/pulse, but the detectors used for the crystal channeling experiment required intensities on the order of 50 fC/pulse. Both of these are well below the sensitivity of the BPMs (~100 pC/pulse), and so running beam for crystal channeling required the beamline to be set, then the beam attenuated by reducing the drive laser UV to the photocathode, first using neutral density filters to achieve a 200 pC/pulse maximum pulse train, then use a combination of a wave plate and UV beam splitting cube to attenuate to a minimum. Bleed-through from the splitter at this level was measured to reliably be ~50 fC/pulse using a Faraday cup at the gun. This is a destructive measurement so it was not continuously monitored, but checked frequently.

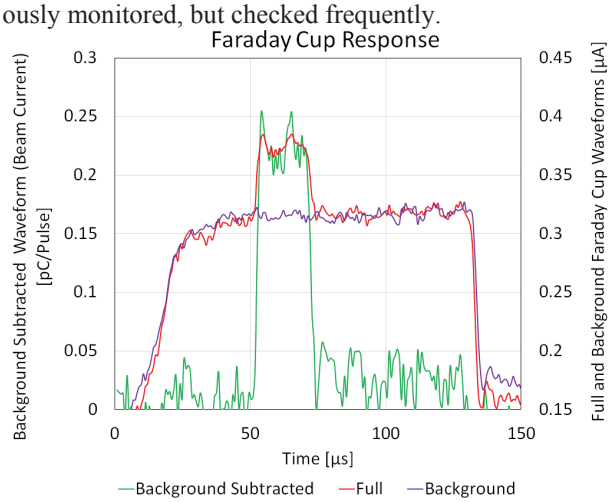

Figure 2: Nominal gun energy is 5 MeV. Reduced dark current gradient was 4.3 MeV for the crystal channeling. A ~200 fC/pulse Faraday cup signal is shown above (green).

At these intensities with a nominal gun gradient of 42 MV/m the dark current, especially from the photoinjector gun, is nominally much greater than the beam intensity. A number of steps were taken to reduce the effect of the dark current including shortening the gun pulse, running the gun at a lower gradient in a trade-off with space-charge effects (see Fig. 2), and scraping through the chicane. Note that the chicane dipoles are not NMR-locked like the spectrometer dipole is.

Stability & CC Transport Matrix Measurement

The stability of the beam was measured with BPMs at various locations along the beamline (see Fig. 3), especially around the two capture cavities. These in particular, along with scans of the dipole correctors H/V100 and H/V101, were used in collecting data to measure the transport matrix through the capture cavities and integrate up- and down-stream Higher Order Mode (HOM) detectors for each cavity into the control system. Analysis of the transport matrix data was recently reported [13]. The BPMs were improved through the 50-MeV run and were used to record a ~60 μm standard deviation of beam positions through most of the beamline due to a combination of beam stability and BPM noise, one known source residing in the same relay rack as the BPM electronics. Further noise reduction is planned for the 150-300 MeV run in 2017.

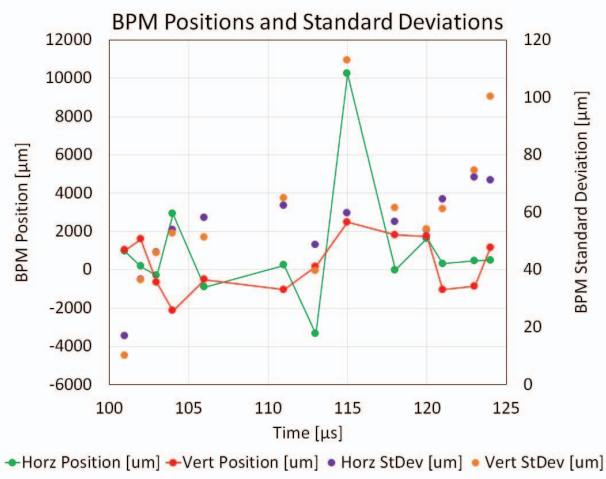

Figure 3: The BPM positions and standard deviations at each BPM location are plotted above.

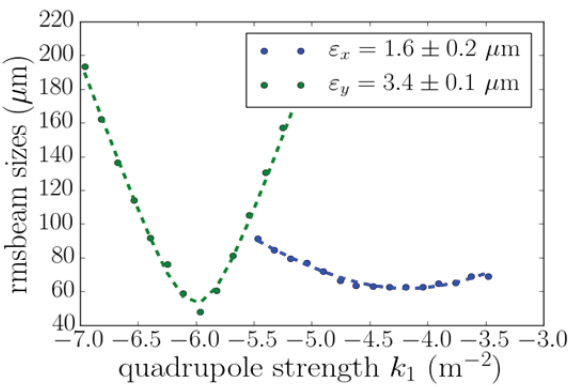

Figure 4: A scan of quadrupole (Q120) strength to measure emittance with horizontal (blue) and vertical (green) fits at the X121 YAG.

Emittance

To measure beam emittance, scans were performed with quadrupoles while the resulting spot changes recorded at a downstream YAG screen. These were evaluated using python routines to determine geometrical and normalized transverse beam emittances from the measured Courant-Snyder parameters, initially for a thin-lens approximation before implementation of a thick-lens model, the latter are noted in Table 1 and shown in Figure 4 [14,15].

Bunch Length

Bunch length measurements were performed on the electron beam using the beamline streak camera. Even at low charge the bunch elongates with increasing space charge. The electron bunch length was measured to be 4.7 ps (an 18% effect over the UV drive laser pulse) for a 60 pC/pulse at X121. Compressing through the chicane by adjusting the CC2 phase, the compressor shortened the pulse to 0.53 ps as seen in Figure 5 [16]. This was also measured with the MPI.

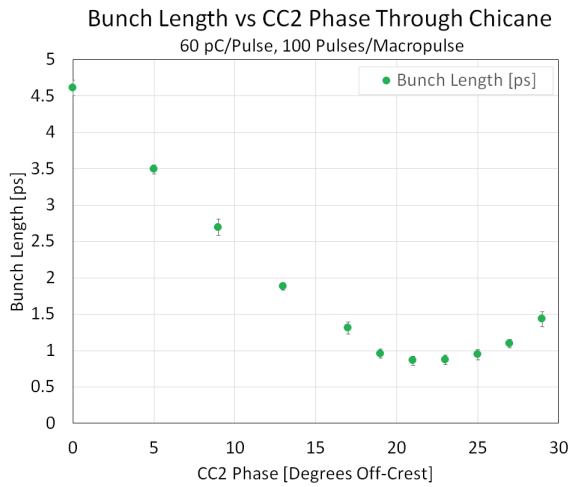

Figure 5: A minimum bunch length was found with the streak camera by adjusting the beam chirp through the CC2 phase for a given bunch compressor skew quadrupole setting and placing a 550 nm longpass filter in-line with the streak camera. The minimum was found at 0.86 ps.

CONCLUSION

The 50-MeV run in the FAST electron injector low-energy beamline was a critical step in providing support for IOTA and high-energy electron activities at the FAST facility in the coming years. In this run, the beamline has been shown to be quite flexible, many extents of its operational space tested in terms of intensity, bunch length, emittance, and bunch stability.

ACKNOWLEDGMENT

We would like to thank everyone helping to make the FAST electron injector a reality, including our colleagues in the APC, the NIU-based crystal channeling team, as well as Accelerator Division and Technical Division support groups. Finally, we owe a debt of gratitude to H. Edwards for her pioneering work in the field of SRF.

REFERENCES

[1] P. Garbincius *et al*., Fermilab-TM-2568 (2013).
[2] V. Danilov, S. Nagaitsev, PRSTAB 13, 084002 (2010).
[3] C. Hall, *et.al*, presented at NA-PAC'16, Chicago, IL, USA, October 2016, paper WEA4CO02, this conference.
[4] A.Burov, W.Foster, V.Shiltsev, Fermilab TM-2125 (2000).
[5] M.McGee, *et al*, in Proc. IPAC'16, p.2271 (2016).
[6] V.Shiltsev, in Proc. IEEE PAC'07, p.1159 (2007).
[7] C.S. Park, *et al*, presented at NA-PAC'16, Chicago, IL, USA, October 2016, paper THA3CO04, this conference.
[8] J.C. Thangaraj, *et al*, "Ceramic Gap Monitor to Measure Bunch Length Non-Invasively in a Superconducting Electron Linac," to be presented at IBIC 2017, Grand Rapids, MI, USA, August 2017, unpublished.
[9] D.J. Crawford, *et al*, in Proc. IPAC'15, Richmond, VA, USA, May 2015, paper TUPJE080.
[10] B.L. Beaudoin, *et al*, in Proc. IPAC'15, Richmond, VA, USA, May 2015, paper MOPMA043.
[11] D. Edstrom, FNAL AD Elog Entry #46158 (internal).
[12] P. Hall, P. Piot, T. Sen, private communication, October 2016.
[13] A. Halavanau, *et al*, presented at LINAC'16, East Lansing, MI, USA, September 2016, paper MOP106018, unpublished.
[14] A. Green, "Development of a Python Based Emittance Calculator at Fermilab Science & Technology (FAST) Facility," Northern Illinois University (2016).
[15] P. Piot, FNAL AD Elog Entry #85886 (internal).
[16] A.H. Lumpkin, *et al*, presented at NA-PAC'16, Chicago, IL, USA, October 2016, paper TUPOA26, this conference.